FERMILAB-PUB-16-366-TD
ACCEPTED

Efficient expulsion of magnetic flux in superconducting radiofrequency cavities for high Q_0 applications

S. Posen,[a] M. Checchin, A. C. Crawford, A. Grassellino, M. Martinello, O. S. Melnychuk, A. Romanenko, D. A. Sergatskov, and Y. Trenikhina
Fermi National Accelerator Laboratory, Batavia, Illinois, 60510, USA.

(Dated: 17 May 2016)

Even when cooled through its transition temperature in the presence of an external magnetic field, a superconductor can expel nearly all external magnetic flux. This paper presents an experimental study to identify the parameters that most strongly influence flux trapping in high purity niobium during cooldown. This is critical to the operation of superconducting radiofrequency cavities, in which trapped flux degrades the quality factor and therefore cryogenic efficiency. Flux expulsion was measured on a large survey of 1.3 GHz cavities prepared in various ways. It is shown that both spatial thermal gradient and high temperature treatment are critical to expelling external magnetic fields, while surface treatment has minimal effect. For the first time, it is shown that a cavity can be converted from poor expulsion behavior to strong expulsion behavior after furnace treatment, resulting in a substantial improvement in quality factor. Microscopic investigations are performed to study the relevant changes in the material from this treatment. Future plans are described to build on this result in order to optimize treatment for future cavities.

I. INTRODUCTION

Recently, concentrated research effort has been devoted to obtaining high quality factors (Q_0) in superconducting radiofrequency (SRF) cavities, structures that transfer energy to beams in particle accelerators. High Q_0 reduces the considerable costs for cryogenics—both infrastructure and AC wall power for the cryogenic plant—required to cool cavities operating with high duty factor. Treatments such as nitrogen-doping[1] have been invented to substantially improve nominal quality factors, but Q_0 can be strongly degraded by trapped magnetic flux.

Q_0 degradation by trapped flux can be considered as a three step process: 1) the cavity is cooled in a finite external magnetic field environment B_{ext}; 2) some of that field, B_{trap}, is trapped in the surface of the cavity; and 3) the surface resistance R_s of the cavity (Q_0 is inversely proportional to R_s) is increased by an amount R_{fl} due to the trapped field. Preparation can be optimized to reduce the impact of each of these steps. Use of non-magnetic components, magnetic shielding, and active field cancellation can reduce B_{ext} in step 1 (see e.g. Ref. 2). The mean free path can be optimized to reduce R_{fl} for a given B_{trap} in step 3 (see e.g. Refs. 3 and 4). For step 2, the amount of external field trapped in the cavity during cooldown can be reduced, and recent experiments have shown that even full expulsion is possible (previous experimental results[5,6] had reported full trapping—$B_{trap} \sim B_{ext}$). These recent experiments include the discovery that the fraction of external field that is trapped in the surface of a niobium cavity during cooldown is strongly dependent on the thermal gradient over its surface[7,8]. This flux expulsion may be caused by thermal diffusion forces[9] exceeding forces attracting flux lines to pinning sites (the present case considers forces on flux lines during cooldown from the critical temperature T_c; see Ref. 10 for experiments well below T_c). Another proposed mechanism involves reducing the opportunities for interaction between flux lines and trapping sites[11]. In this paper, we present an experimental study that further develops the understanding of flux expulsion in niobium cavities. For the first time, expulsion is studied as a function of both thermal gradient and cavity preparation. The goal of the study was to determine whether flux trapping behavior is determined by bulk properties (e.g. grain boundaries, as in Refs. 12 and 13; see also Ref. 14) or surface properties (e.g. nitrides from the nitrogen-doping process[15]; see also Refs. 16 and 17) and then to find a treatment that improves expulsion.

The arrangement for measuring flux expulsion in a single cell cavity is shown in Figure 1 (measurement technique from Ref. 7). Magnetic field coils are arranged around the cavity, and a current is applied to create a field of ∼10 mG at the surface. Fluxgate magnetometers are attached to the middle of the cavity cell, oriented in the same direction as the applied field. Thermometers measure the temperature at the top, bottom, and middle of the cavity cell. During cooldown, as the temperature falls below the transition temperature T_c and the cavity goes from the normal conducting (NC) state to the superconducting (SC) state, a step change is observed in the magnetic field data. The magnitude of this change corresponds to the amount of flux expelled. If B_{ext} is fully trapped, the field measured above T_c, B_{NC}, is the same as the field measured below T_c, B_{SC} (B_{SC}/B_{NC}=1). When B_{ext} is completely expelled, calculations of the full Meissner expulsion show that the expected[18] ratio of B_{SC}/B_{NC} should be 1.7. In this way, the measurement of B_{SC}/B_{NC} reveals what fraction of flux is trapped during cooldown instead of being expelled. The temperature difference between the top and bottom thermometer at

[a] Electronic mail: sposen@fnal.gov

Operated by Fermi Research Alliance, LLC under Contract No. DE-AC02-07CH11359 with the United States Department of Energy.

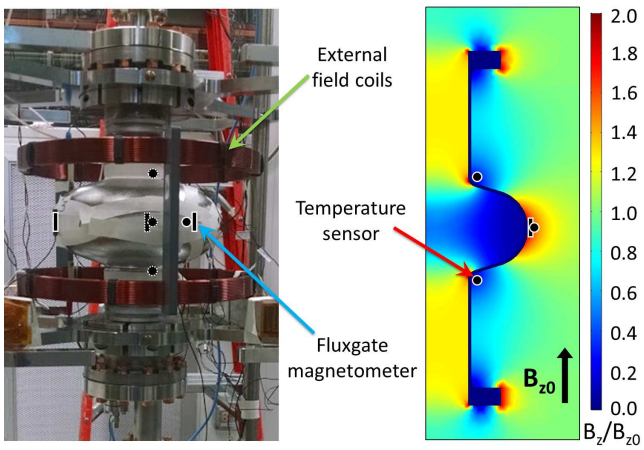

FIG. 1. Apparatus for measuring magnetic flux expulsion in a 1.3 GHz single cell SRF cavity (left), and simulation of axial field component B_z resulting from the complete expulsion of an external field $\mathbf{B_{z0}}$ parallel to the cavity axis, normalized to B_{z0} (right).

T_c gives a measure of the temperature gradient across the cavity. Typical measurements[19] of flux expulsion are shown in Figure 2.

II. MAGNETIC MEASUREMENTS

Several single cell 1.3 GHz cavities were measured over a number of cooldown cycles to show the trend with temperature gradient for a given cavity preparation. A total of 24 datasets were obtained, each for a different treatment. Each dataset consists of many cooldowns to ∼7 K, varying ΔT (cold helium enters the dewar from below, providing intense cooling to the bottom of the cavity, such that higher starting temperatures lead to larger ΔT values when the cavity reaches 9 K). A trend in the data quickly became apparent, as shown in Figure 3. Two production groups of cavities from the same vendor had consistently different trapping behavior: the cavities from production group 1 expelled well while those in production group 2 expelled poorly. For the cavities that expel flux well, ΔT as low as 2 K over the cavity cell are sufficient to expel the majority of the external field. For the cavities that expel poorly, the majority of the flux is trapped even for ΔT close to 10 K.

The cavities in production group 1 showed another notable behavior. The cavities in this production group, which were made from material with grain size ∼100 µm, exhibited extensive grain growth after the standard processing steps, which includes ultra-high-vacuum (UHV) furnace treatment at 800°C for several hours (all cavities shown in Fig. 3 were treated with similar integrated times at 800°C of between 3-7 h, with the exception of AES09, with an integrated time of ∼18 h). This is illustrated in Figure 4, showing grains that have grown as large as a few mm. These cavities consistently had significantly larger grains than those in production group 2, which showed weaker flux expulsion behavior. Cavities from other production groups also show similar correlations. Figure 5 shows two fine grain cavities that expel poorly and one large grain cavity that expels well.

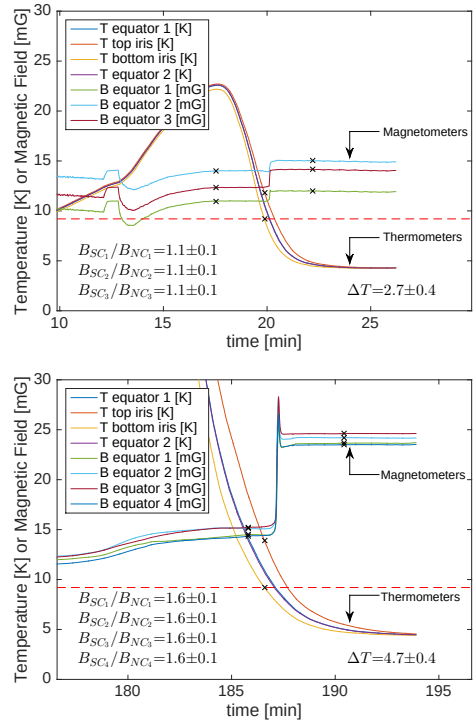

FIG. 2. Typical flux expulsion measurements. As the cavity passes through T_c during cooldown (dashed line), temperature and magnetic field are recorded (illustrated with 'x' symbols). Some cavity preparations can result in strong flux trapping behavior, showing B_{SC}/B_{NC} ratios close to 1 for modest ΔT (e.g. top) and others result in efficient flux expulsion, with ratios close to 1.7 under similar conditions (e.g. bottom).

One of the cavities from production group 2 was heated at 1000°C for 4 hours in a UHV furnace. If modification of the bulk crystal structure—e.g. grain size, dislocation content—was the effect that led to strong flux expulsion in production group 1, this would be expected to improve this property in production group 2. The results are shown in Figure 6, including a visible increase in grain size and a substantial improvement in flux expulsion.

Shorter and lower temperature furnace treatments were investigated as well. Fig. 7 shows two cavities from production group 2, that were converted to expel strongly after treatments at 1000°C for 1 hours and 900°C for 3 hours. In both cases, expulsion is greatly improved compared to when the cavity had only been treated at 800°C for several hours, and the impact appears to be stronger for the cavity that received 1000°C treatment.

The cavities measured in the survey had been treated

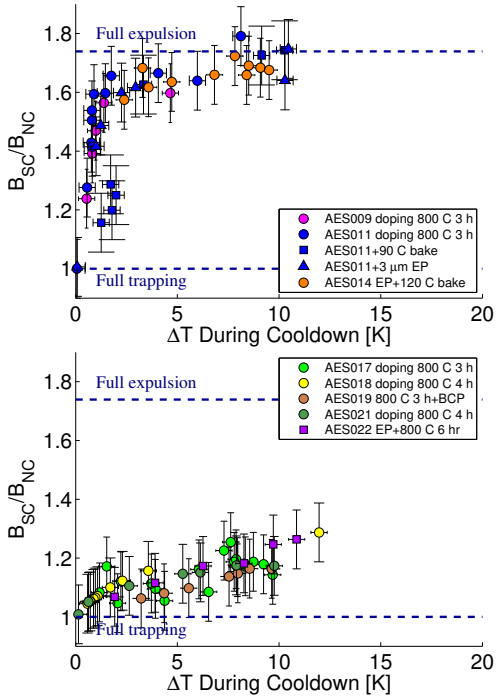

FIG. 3. Measured curves of flux expulsion as a function of temperature difference ΔT from bottom to top of the cavity cell as the cavity passes through T_c during cooldown. The cavities measured from production group 1 (AES007-AES016) showed strong expulsion behavior (top) while those from production group 2 (AES017-AES022) showed strong trapping (bottom). The cavities within a production group showed similar behavior in spite of different preparations.

FIG. 4. Grain growth in AES011. The cavity was fabricated from material with ∼100 μm sized grains, some of which grew to the few mm-scale after only a few UHV furnace cycles at 800°C that were each 3 hours long or shorter.

with a wide variety of surface processing techniques. By comparing cavities from the same production group, with similar furnace treatment history but different surface processing, we can study the effect of the surface on flux expulsion. We can also study the effect of a given surface treatment by comparing flux expulsion on a single cavity

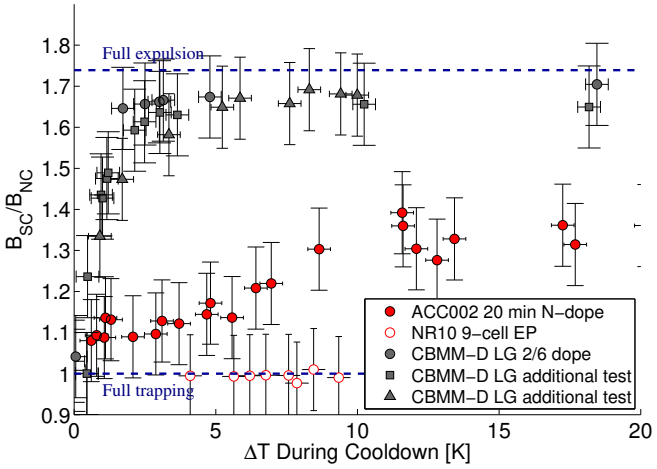

FIG. 5. Flux expulsion measurement in two 1.3 GHz fine grain cavities, single cell ACC002 and 9-cell NR010, and one large grain 1.3 GHz single cell, CBMM-D. It should be noted that CBMM-D received more furnace cycles than ACC002 or NR010.

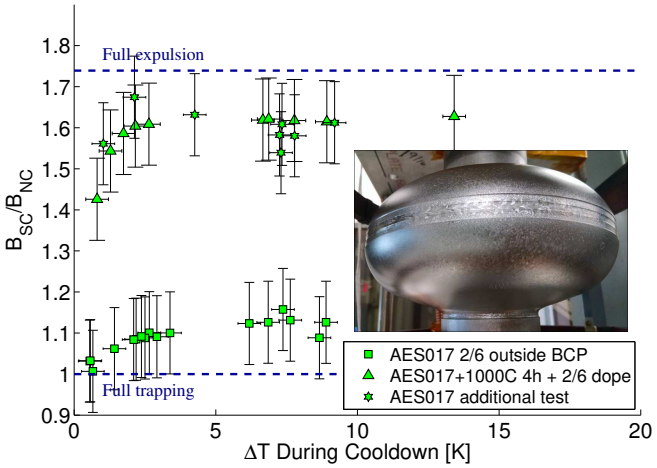

FIG. 6. AES017, a cavity from production group 2 that showed strong flux trapping behavior, was converted to expel strongly after a 1000°C 4 h furnace treatment. The inset image shows the grain growth after treatment.

before and after treatment. Figure 8 shows a number of such comparisons, such as electropolished (EP) surface vs buffered chemical polish (BCP) surface, nitrogen-doping with "2/6" recipe (see Refs. 1 and 15 for information on the nitrogen-doping process and 2/6 recipe) vs EP, and as-treated outside surface vs outside BCP. In each case, the flux expulsion is nearly the same for cavities with similar bulk history regardless of surface conditions.

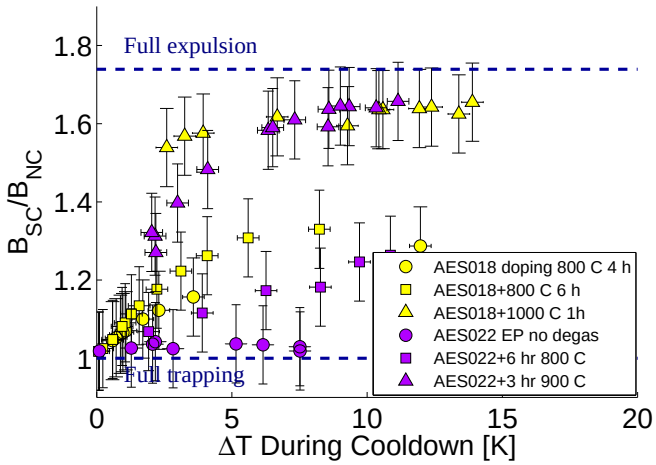

FIG. 7. AES018 and AES022, two cavities from production group 2 that showed strong flux trapping behavior, were converted to expel strongly after, respectively, a 900°C 3 h and 1000°C 1 h furnace treatment.

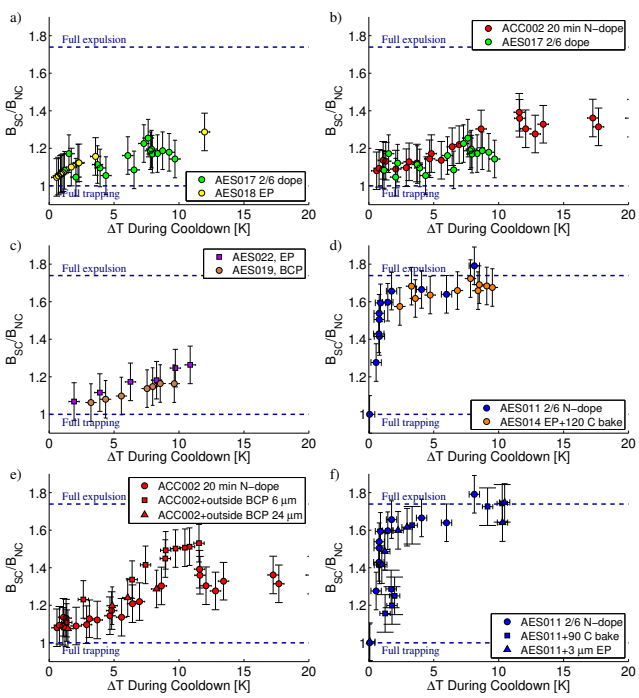

FIG. 8. Flux expulsion vs ΔT, comparing a variety of different surface treatments with similar bulk history. Each graph compares curves for 2 or 3 treatments that produce very different surfaces but show similar expulsion behavior: a) EP vs N-doped; b) 'light' N-dope (20 minutes in N at 800°C) vs 'heavy' N-dope (2 minutes in N at 800°C + 6 minute anneal); c) EP vs BCP; d) light doping + external BCP vs EP + 120°C bake; e) effect of light and heavy BCP of external surface (same cavity) f) effect of 90°C bake and additional EP (same cavity).

III. RF MEASUREMENTS

To show that flux expulsion significantly affects Q_0, RF measurements were performed on the cavity from Figure 6 before and after 1000°C furnace treatment. Each time, the cavity was cooled down in a 10 mG field with a modest ΔT of 2-4 K. The B_{SC}/B_{NC} ratio measured before heat treatment was 1.1, showing that most of the external flux was trapped, while the ratio measured after was 1.6, showing strong expulsion (these cooldowns are shown in Figure 2). Figure 9 shows the corresponding substantial improvement[20] in Q_0 at 1.5 K and 2 K. The substantial Q-slope observed after furnace treatment is not expected to be related to the flux expulsion mechanism (based on similar cavities that expelled well) nor to the grain growth (based on experience with large grain cavities). Rather, it is believed to be due to contamination from the furnace, based on observations of other cavities treated in a similar timeframe.

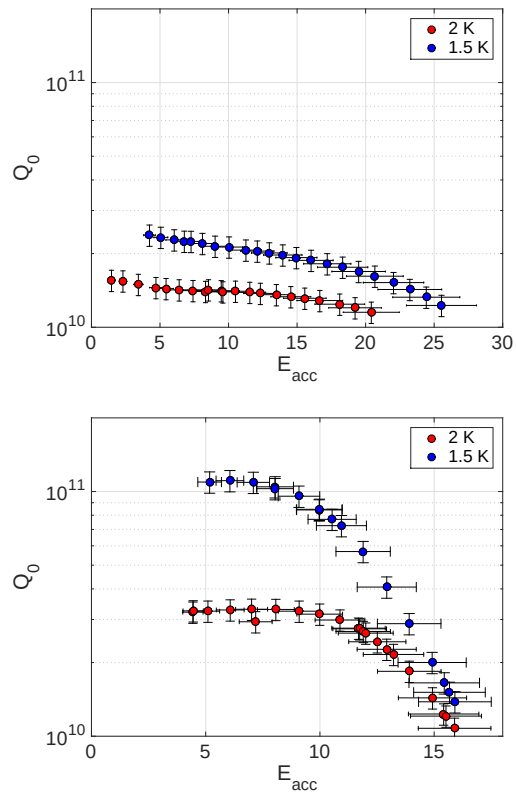

FIG. 9. Q_0 vs accelerating gradient E_{acc} for AES017 after cooldown in a 10 mG field with a modest ΔT ∼2-4 K. Before 1000°C heat treatment (top), the cavity traps most of the flux and resulting in a low field Q_0 at 1.5 K of $\sim 2 \times 10^{10}$. After the heat treatment to improve flux expulsion (bottom), this value improves to $\sim 1 \times 10^{11}$.

IV. MICROSCOPIC MEASUREMENTS

For cavities that received the 900°C and 1000°C treatments, with results shown in Fig. 7, niobium witness samples were treated along with the cavities[21]. Using a microscope with electron backscatter detection (EBSD) capabilities[22,23], these samples were analyzed for crystal orientation, as were samples that were not given furnace treatment. Fig. 10 shows an EBSD crystal orientation map, using a local misorientation angle of 10° to distinguish grain boundaries. It can be seen that an increase in grain size is observed after high temperature treatment, with the largest effect after 1000°C treatment.

Fig. 11 shows maps of local misorientation angle, which is related to dislocation content[22,24]. Fig. 12 presents histograms of the local misorientation angle data for each map. Note that after furnace treatment, the peak at relatively small misorientation angles, ∼0.2° is increased, accompanied by a reduction in the tail at higher misorientation angles. The overall effect is that somewhat smaller misorientation angles are observed on average.

V. DISCUSSION

Magnetic measurements showed that for cavities that exhibited poor expulsion, high temperature treatment at 900-1000°C produced a substantial improvement in flux expulsion and increased grain size. This points to bulk structure as the source of flux trapping during cooldown; for example, if grain boundaries act as strong pinning sites for flux near T_c, cavities with more grain boundaries would be expected to trap more strongly. Previous experiments on niobium samples studied the difference between fine grain (tens of µm grain size) and large grain (mm-scale grain size) material in fraction of flux trapped during cooldown[25,26]. These studies were performed before it was recognized that it was important to control for thermal gradient, making it difficult to extract quantitative data, but qualitative trends were demonstrated. Material with larger grains appeared to have higher expulsion, which is consistent with the results in Figure 3, as well as with previous studies of high field pinning[12,13]. However, even in single crystal niobium samples, heat treatment appeared to improve expulsion, suggesting that crystal properties other than grain boundaries (e.g. dislocations) play an important role[25].

We can apply a simple model to attempt to predict the quality factor that would be achieved in the cavities from production groups 1 and 2, depending on the temperature gradient applied during cooldown (converting from ΔT using the approximate distance between thermometers of 20 cm). This model will require a number of assumptions that will not apply in every situation, but can provide a helpful case study. First, an exponential decay function is used to fit the B_{SC}/B_{NC} vs ΔT data

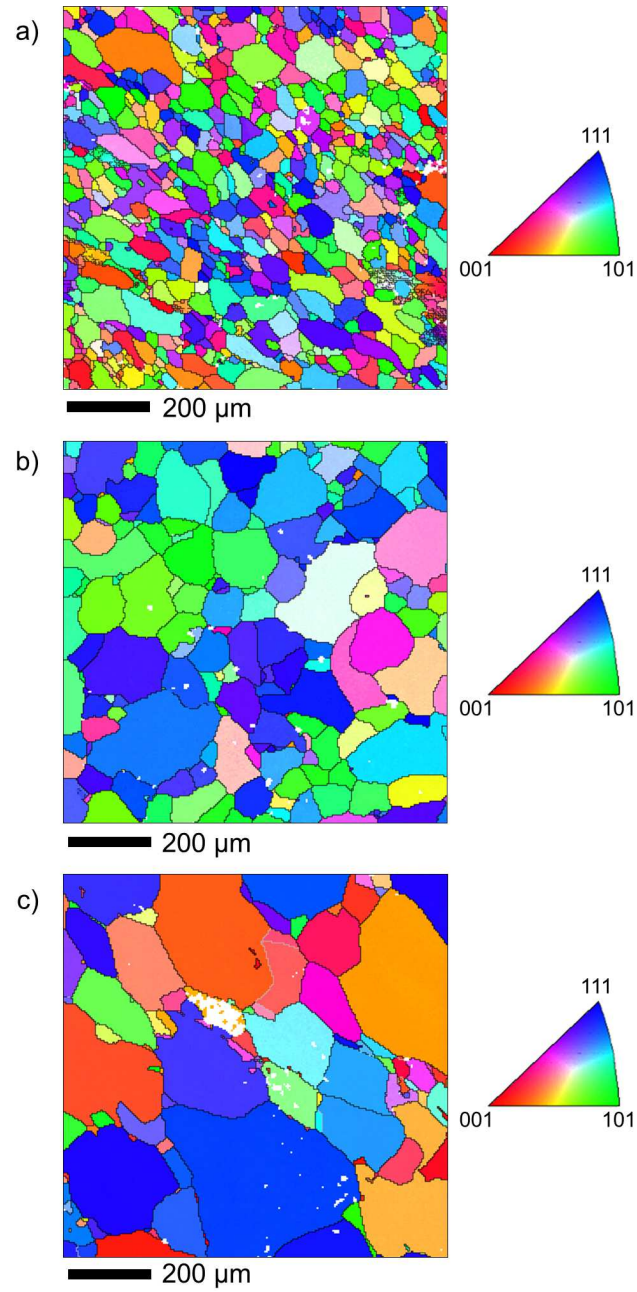

FIG. 10. Crystal orientation maps of niobium samples with three different treatments: a) as received, b) treatment at 900°C for 3 hours (with AES022), c) treatment at 1000°C for 1 h (with AES018). Significant grain growth is observed in cases b) and c). Some pixels could not be indexed and are shown in white.

from Fig. 3, and the trapped flux B_{trap} relative to the applied field B_{z0} is calculated assuming that the fraction of flux trapped changes linearly between full trapping at B_{SC}/B_{NC}=1 and full expulsion at 1.7. Then the added surface resistance due to trapped flux is calculated from $R_{fl} = \eta \frac{B_{trap}}{B_{z0}} B_{z0}$, where η is the sensitivity

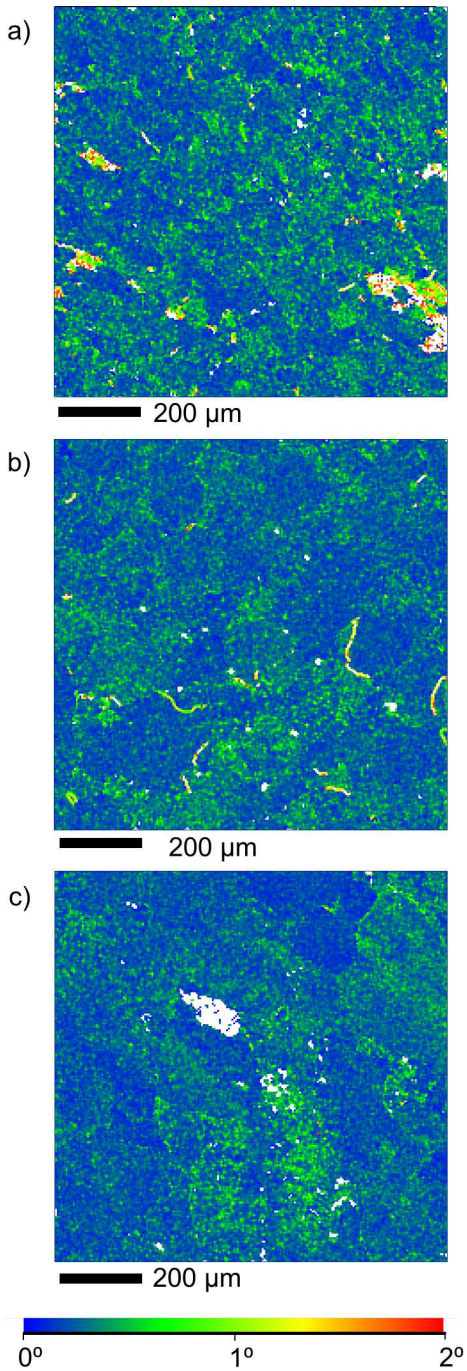

FIG. 11. Maps of local misorientation angle (which is related to dislocation content) for the same areas shown in Fig. 10. White pixels either are out of range or could not be indexed.

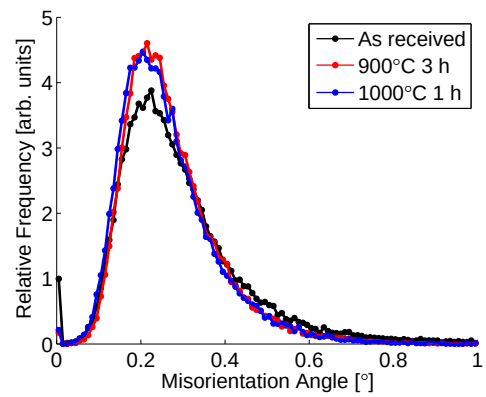

FIG. 12. Histograms of local misorientation angle data from Fig. 11. Somewhat smaller misorientation angles are observed after furnace treatment.

to trapped flux, approximately 1.1 nΩ/mG for cavities treated with the 2/6 nitrogen-doping procedure based on previous measurements[3]. Then an overall Q_0 is calculated as a function of ΔT assuming a certain baseline surface resistance to which R_{fl} is added. So that we can compare to data, we choose a resistance of 7.7 nΩ, which was measured for AES017 at 2 K and 5 MV/m after 1000 C bake, when it was cooled with a large ΔT in an external field <1 mG, such that R_{fl} should be very small. Finally, ΔT is converted to a temperature gradient, using the length along the cavity surface between the two thermometers. The resulting plot is shown in Fig. 13, for several different applied fields. The model predicts a substantial degradation in Q_0 for production group 1 when cooling in applied fields even as low as 5 mG. The RF data points collected for AES017 at 5 MV/m over several tests are also plotted on the graph, including data collected after 1000 C bake, when the expulsion behavior is similar to that of the cavities of production group 1. Good agreement is shown between the data and this model. It should be noted that a) the field B_{z0} measured by the fluxgates at transition was measured to be 10±5 mG in these experiments (variation may be caused by temperature fluctuations in magnetic shielding), b) the exponential function fits the data from Fig. 3 well, but it may not be the correct function to use, c) the parameters here provide a helpful illustration, but other production groups will yield different baseline resistances and expulsion characteristics.

If grain boundaries were acting as strong flux pinning sites, it would be consistent with previously reported results of significantly improved quality factors in large grain cavities compared to fine grain cavities[27,28].

Microscopic measurements revealed that the 1000°C treatment for 1 h produced larger grains than the 900°C treatment for 3 h. If grain size were a determining factor for flux expulsion, this would be consistent with the reduced ΔT that gives near-full flux expulsion after the 1000°C treatment compared to the 900°C treatment. The local misorientation angle is observed to decrease somewhat after furnace treatment, though the correlation with flux expulsion is not as evident. Additional studies are needed to determine the impact of dislocation content. Continued experiments are planned on samples,

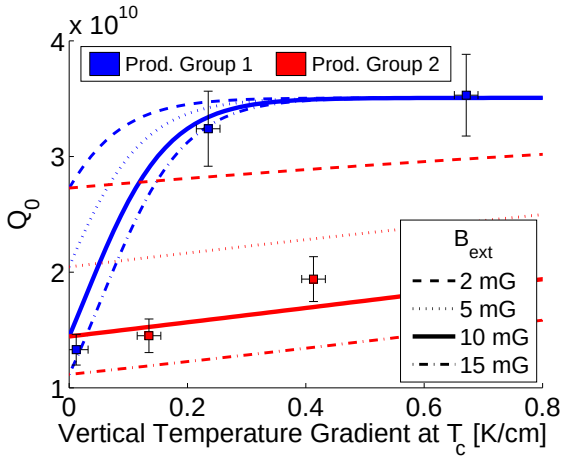

FIG. 13. A simple model is used to calculate Q_0 at 2 K and 5 MV/m as a function of temperature gradient during cooldown for a number of applied fields. Substantial Q_0 degradation is predicted for production group 2 (red lines), which showed poor expulsion compared to group 1 (blue lines). Data measured from AES017 cooled in a 10±5 mG field before (red squares) and after (blue squares) 1000 C treatment shows good agreement (compare to solid lines).

including comparisons of the materials from production groups 1 and 2, grain size and local misorientation angle measurements after treatments with different temperatures and durations, and tensile testing.

These experiments studied single cell cavities that were cooled in a dewar with their axes in the vertical orientation. In contrast, high Q_0 accelerator applications generally use multicell cavities in horizontal orientation, with their helium jackets connected together in long strings. Previous experiments[29,30] have shown that in the horizontal cavity orientation, vertical thermal gradients—in this case, perpendicular to the cavity axis—are beneficial to flux expulsion (consistent with what is observed in the experiments presented here). For example, in the upcoming LCLS-II project[31], a high duty factor accelerator where obtaining high Q_0 is critical to minimizing cryogenic costs, the specification for magnetic field in the cryomodules is 5 mG. As Fig. 13 illustrates, cavities that trap flux from a 5 mG field during cooldown could be vulnerable to significant Q_0 degradation. In order to maximize flux expulsion, each cryomodule will have its own set of cryogenic valves to provide a high flowrate of cold helium to the bottom of the cavities during cooldown, and therefore increase the vertical temperature gradient[32]. However, just as in vertical test, there will be limitations on the thermal gradient that can practically be achieved, which may limit the expelled flux, depending on the cavity material. For material that behaves like production group 2, a 900-1000°C heat treatment step could encourage strong flux expulsion and substantially improve the Q_0 that can be achieved with realistic background magnetic fields and temperature gradients during cooldown.

VI. CONCLUSIONS

In this paper, we have presented new results measuring expulsion of magnetic flux during cooldown through T_c in niobium SRF cavities. It was found that efficient flux expulsion is strongly influenced not only by thermal gradient but also by treatment. Cavities that showed signs of modified bulk structure after high temperature furnace treatment exhibited significantly stronger flux expulsion as a function of temperature than those that did not. The surface preparation showed no significant effect. Using these results, a procedure was designed that demonstrated substantial improvement in flux expulsion behavior via UHV furnace treatment at 900-1000°C. A 1.3 GHz cavity was evaluated before and after treatment at 1000°C for 4 h by cooling in a field ∼10 mG with a modest temperature gradient ∼2-4 K. After 1000°C treatment, RF measurements showed that Q_0 at 1.5 K improved by a factor of ∼5. Preliminary microscopic studies studying what specific properties determine expulsion behavior showed a correlation between increased grain size and improved flux expulsion at smaller thermal gradients, but additional studies are required.

Future work will focus on optimizing treatment for improving flux expulsion without compromising mechanical properties. For example, if grain boundary density is important to expulsion behavior, future cavities could be manufactured from material with larger grain size, or cavities could be given an optimized furnace treatment after manufacture to ensure that high Q_0 can be maintained in a cryomodule environment with a realistic background magnetic field.

The experimental results presented here may be useful in other applications where magnetic field isolation is important, such as in quantum computing.

This work was supported by the United States Department of Energy, Offices of High Energy and Nuclear Physics. The authors are grateful for technical assistance from the FNAL cavity preparation and cryogenic teams. Fermilab is operated by Fermi Research Alliance, LLC under Contract No. DE-AC02-07CH11359 with the United States Department of Energy.

[1] A. Grassellino, A. Romanenko, D. Sergatskov, O. Melnychuk, Y. Trenikhina, A. Crawford, A. Rowe, M. Wong, T. Khabiboulline, and F. Barkov, Supercond. Sci. Technol. **26**, 102001 (2013).
[2] D. A. Edwards (ed.), "TESLA Test Facility (TTF) Linac Conceptual Design Report," Tech. Rep. Ch. 4 (1995).
[3] M. Martinello, M. Checchin, A. Grassellino, O. Melnychuk, S. Posen, A. Romanenko, D. Sergatskov, and J. F. Zasadzinski, Proc. Seventeenth Int. Conf. RF Supercond. **MOPB015** (2015).
[4] D. Gonnella, J. Kaufman, and M. Liepe, arXiv: 1509.04127 (2015).
[5] H. Padamsee, J. Knobloch, and T. Hays, *RF superconductivity for accelerators* (Wiley-VCH, New York, 2008) p. 521.
[6] C. Vallet, M. Bolore, B. Bonin, J. P. Charrier, B. Daillant, J. Gratadour, F. Koechlin, and H. Safa, Proc. EPAC 1992 , 1295 (1992).
[7] A. Romanenko, A. Grassellino, O. Melnychuk, and D. A. Sergatskov, J. Appl. Phys. **115**, 184903 (2014).

[8] A. Romanenko, A. Grassellino, A. C. Crawford, D. A. Sergatskov, and O. Melnychuk, Appl. Phys. Lett. **105**, 234103 (2014).
[9] R. P. Huebener and A. Seher, Phys. Rev. **181**, 701 (1969).
[10] G. Ciovati and A. Gurevich, Phys. Rev. Spec. Top. - Accel. Beams **11**, 122001 (2008).
[11] T. Kubo, arXiv: 1601.02118 (2016).
[12] A. Dasgupta, C. C. Koch, D. M. Kroeger, and Y. T. Chou, Philos. Mag. Part B **38**, 367 (1978).
[13] A. T. Santhanam, J. Mater. Sci. **11**, 1099 (1976).
[14] T. Tai, B. G. Ghamsari, T. Bieler, and S. M. Anlage, Phys. Rev. B - Condens. Matter Mater. Phys. **92**, 134513 (2015).
[15] A. Grassellino, A. Romanenko, S. Posen, Y. Trenikhina, O. Melnychuk, D. Sergatskov, M. Merio, M. Checchin, and M. Martinello, Proc. Seventeenth Int. Conf. RF Supercond. , MOBA06 (2015).
[16] Z.-H. Sung, A. Dzyuba, P. J. Lee, D. C. Larbalestier, and L. D. Cooley, Supercond. Sci. Technol. **28**, 075003 (2015).
[17] G. Ciovati, G. Myneni, F. Stevie, P. Maheshwari, and D. Griffis, Phys. Rev. Spec. Top. - Accel. Beams **13**, 022002 (2010).
[18] The calculation of B_{SC}/B_{NC} for full expulsion takes into account the thickness of the fluxgate probe but not its length, and it assumes that the probe is ideally centered at the equator. Calculations show that the effect of these factors is expected to be $< 5\%$, and they are omitted in the figures for simplicity.
[19] Sources of measurement uncertainty in ΔT include thermal impedance between cavity and thermometer, assumed to result in overall uncertainty of 0.4 K. Sources of measurement uncertainty in B_{SC}/B_{NC} include radial background fields and misalignment of fluxgate probe, assumed to result in overall uncertainty of 0.1.
[20] An uncertainty of 10% is assumed for Q_0 and E_{acc} measurements.
[21] The witness samples were made with the excess high RRR niobium material from the fabrication of production group 2 cavities (AES017-AES022).
[22] O. S. Romanenko, PhD Thesis, Cornell Univ. (2009).
[23] D. Kang, D. C. Baars, T. R. Bieler, and C. C. Compton, AIP Conf. Proc. **1352**, 90 (2011).
[24] D. P. Field, P. B. Trivedi, S. I. Wright, and M. Kumar, Ultramicroscopy **103**, 33 (2005).
[25] S. Aull, O. Kugeler, and J. Knobloch, Phys. Rev. Spec. Top. - Accel. Beams **15**, 062001 (2012).
[26] A. S. Dhavale, P. Dhakal, A. A. Polyanskii, and G. Ciovati, Supercond. Sci. Technol. **25**, 065014 (2012).
[27] W. Singer, S. Aderhold, A. Ermakov, J. Iversen, D. Kostin, G. Kreps, A. Matheisen, W. D. Mueller, D. Reschke, X. Singer, K. Twarowski, H. Weise, and H. G. Brokmeier, Phys. Rev. Spec. Top. - Accel. Beams **16**, 012003 (2013).
[28] A. Navitski, Proc. Ingot Niobium Work. (2015).
[29] M. Martinello, M. Checchin, a. Grassellino, a. C. Crawford, O. Melnychuk, a. Romanenko, and D. a. Sergatskov, J. Appl. Phys. **118**, 044505 (2015).
[30] D. Gonnella, R. Eichhorn, F. Furuta, M. Ge, D. Hall, V. Ho, G. Hoffstaetter, M. Liepe, T. O'Connell, S. Posen, P. Quigley, J. Sears, V. Veshcherevich, A. Grassellino, A. Romanenko, and D. A. Sergatskov, J. Appl. Phys. **117**, 023908 (2015).
[31] J. N. Galayda (ed.), "LCLS-II Final Design Report, LCLSII-1.1-DR-0251-R0," (2015).
[32] T. Peterson, E. Daly, and J. Preble, "Cryomodule Cool-down Process, LCLSII-4.5-EN-0479-R0," (2015).